

Article

Improving the Powder Properties of an Active Pharmaceutical Ingredient (Ethenzamide) with a Silica Nanoparticle Coating for Direct Compaction into Tablets

Tatsuki Tadauchi, Daiki Yamada, Yoko Koide, Mayumi Yamada, Yasuhiro Shimada, Eriko Yamazoe , Takaaki Ito and Kohei Tahara *

Laboratory of Pharmaceutical Engineering, Gifu Pharmaceutical University, Gifu 501-1196, Japan

* Correspondence: tahara@gifu-pu.ac.jp; Tel.: +81-58-230-8100; Fax: +81-58-230-8105

Abstract: To improve the powder properties of active pharmaceutical ingredients (APIs), we coated APIs with silica nanoparticles using a dry process that allowed for direct compression into tablets. The dry coating performed with different apparatuses (a batch-type high-speed shear mixer (Mechanomill) and a continuous conical screen mill (Comil)) and properties of the resulting dry-coated APIs were compared. Ethenzamide (ETZ), which has low powder flowability, was selected as the host particle to be improved and the colloidal silicas Aerosil 200 and R972 were used as the guest particles. Both coating processes and types of silica nanoparticles improved the powder flowability (angle of repose) of ETZ under unstressed conditions. Inverse gas chromatography demonstrated that dry coating with silica nanoparticles reduced the surface free energy and improved the homogeneity of the surface energy distribution of ETZ particles. Under the stress conditions of a shear cell test, the Mechanomill-based treatment improved the powder flowability of ETZ from that of untreated ETZ; however, the Comil-based treatment did not improve the flowability. The mechanical shear force exerted by Comil was apparently insufficient for interactions between host and guest particles. However, the properties of tableted ETZ were enhanced even when the silica nanoparticles were coated using Comil.

Keywords: dry coating; Comil; ethenzamide; silica nanoparticles; powder flowability



Citation: Tadauchi, T.; Yamada, D.; Koide, Y.; Yamada, M.; Shimada, Y.; Yamazoe, E.; Ito, T.; Tahara, K. Improving the Powder Properties of an Active Pharmaceutical Ingredient (Ethenzamide) with a Silica Nanoparticle Coating for Direct Compaction into Tablets. *Powders* **2022**, *1*, 231–242. <https://doi.org/10.3390/powders1040016>

Academic Editor: Paul F. Luckham

Received: 25 August 2022

Accepted: 2 November 2022

Published: 21 November 2022

Publisher's Note: MDPI stays neutral with regard to jurisdictional claims in published maps and institutional affiliations.



Copyright: © 2022 by the authors. Licensee MDPI, Basel, Switzerland. This article is an open access article distributed under the terms and conditions of the Creative Commons Attribution (CC BY) license (<https://creativecommons.org/licenses/by/4.0/>).

1. Introduction

Pharmaceutical tablets are primarily manufactured by dry granulation, wet granulation, or direct compression [1]. Direct compression is achieved at a lesser cost within a shorter time than granulation processes but is sensitive to the powder properties (such as flowability, die fillability, and compressibility) of the non-granulated active pharmaceutical ingredients (APIs) [2]. In recent years, the particle sizes of many APIs have been reduced to facilitate dissolution, thus, resulting in poor bulk powder properties, such as low flowability, high adhesion, and cohesion [3]. In general, small particles, sized tens of microns, have a large specific surface area, causing adhesion to the surface and aggregation to neighboring particles.

The manufacturing classification system documented the physicochemical properties of APIs that are ideal for direct compression [1,4]. Before direct compaction, the inferior and variable properties of APIs should be improved more simply and less expensively than by general granulation.

Glidants and lubricants, such as talc, magnesium stearate, and silicon dioxide (colloidal/fumed silica), can improve the flowability of API powders [5,6]. Glidants act as spacers between API particles and improve their flowability by decreasing their van der Waals forces. Generally, mechanical shear forces are required for the homogeneous dispersion and adhesion of glidant particles to the API crystal surface (dry nanocoating) [7–9]. Dry nanocoating improves the flowability and compressibility of formulated powders containing excipients. Specialized dry powder processing equipment, such as mechanofusion

and hybridizer machines, generates chemical and physical surface interactions between host and guest particles [10]. However, such specialized dry coating equipment has not been widely adopted in the pharmaceutical industry.

Some recent attempts have fabricated dry powder coatings using conical screen mills (Comil[®], Powrex Corporation, Itami, Japan), the powder processing equipment that sizes granules before the tableting stage in the pharmaceutical industry [11–14]. Comil is capable of continuous powder coating, consistent with the modern concept of continuous production processes [15]. To improve the conventionality and practicality of dry coating of silica nanoparticles by Comil for manufacturing purposes, we must increase the number of successful cases using various APIs and clarify the properties of the API/silica composites.

This study examines the effects of two types of equipment—a batch-type high-speed shear mixer (Mechanomill, Okada Seiko Co., Ltd., Tokyo, Japan) [16] and a Comil screen mill—on the properties of API powders after dry nanocoating (Figure 1). The host particles of ethenzamide (ETZ), a model API with poor flowability, were impregnated with two types of guest particles (silica nanoparticles), hydrophilic Aerosil 200 (A200) and hydrophobic Aerosil R972 (R972) [17,18]. The effects of silica nanoparticle type and dry-coating process on the surface and powder properties of the APIs were then examined. Formulated powders containing dry-coated ETZ with silica nanoparticles were directly compressed to evaluate the impact of Comil dry coating on the manufacturing process and tablet properties.

a) Mechanomill (Batch process)



b) Comil (Continuous process)



Figure 1. Images of (a) Mechanomill and (b) Comil equipment used for the dry coating of silica nanoparticles on active pharmaceutical ingredients. In each panel, the white circle in the left image delineates the powder-processing area of each machine (right photograph).

2. Materials and Methods

2.1. Materials

ETZ was purchased from Iwaki Seiyaku (Tokyo, Japan). A200 and R972 were provided by Nippon Aerosil (Tokyo, Japan). Pharmatose 100M (lactose monohydrate) was provided by DFE Pharma (Nörten-Hardenberf, Germany). Ceolus PH 101 (microcrystalline

cellulose) was provided by Asahi Kasei Corporation (Tokyo, Japan). Magnesium stearate was obtained from Kishida Chemical Co., Ltd. (Osaka, Japan).

2.2. ETZ with Silica Nanoparticles Dry Coated by the Mechanomill

A mixed powder (99/1 *w/w*) of ETZ and silica nanoparticles was sheared at 2000 rpm for 1 min by a Mechanomill (Okada Seiko Co., Ltd., Tokyo, Japan, Figure 1a), thus, resulting in a batch of ETZ dry coated with silica nanoparticles.

2.3. ETZ with Silica Nanoparticles Dry Coated by the Comil

Silica nanoparticles were then dry coated on API by the Comil mixer, which is typically used for disaggregating bulk powders and sizing granules in pharmaceutical manufacturing processes (Figure 1b). ETZ and silica powder (99/1 *w/w*) were mixed in a small-scale V-blender (Tsutsui Scientific Instruments, Tokyo, Japan) at 30 rpm for 4 min. The mixed powder was manually fed into the Comil QC-197S screening mill (Powrex Corporation, Itami, Japan) with an open mesh screen (screen hole diameter = 610 μm) and a round-edged impeller operated at 2000 rpm (impeller tip speed = 2.4 m/s).

2.4. Particle Characterization

The particle shapes were observed by scanning electron microscopy (SEM) (JCM-7000 NeoScope™, JEOL, Tokyo, Japan) at an accelerating voltage of 5–10 kV. For SEM, the samples were sputter coated with metal using a sputter coater (DII-29010SCTR Smart Coater, JEOL). The particle sizes were determined using a laser diffraction particle size analyzer (LDSA) (LDSA-SPR 3500A, MicrotracBEL, Osaka, Japan) equipped with a dry dispersing apparatus.

2.5. Surface Energy Measurements by Inverse Gas Chromatography

Surface energy measurements were performed using inverse gas chromatography (IGC) (iGC-SEA, Surface Measurement Systems, London, UK) [19,20]. The powder was carefully packed in a silanized glass column (300 mm long, 4 mm inner diameter). Both ends of the column were sealed using silanized glass wool (Sigma-Aldrich). Six solvents, hexane, heptane, octane, nonane, dichloromethane, and toluene, were used as nonpolar and polar probes. The surface energies of powder samples were measured at 0% relative humidity (RH) and 30 °C. The carrier gas was helium (10 mL/min flow rate) and the reference gas for injection was methane.

2.6. Powder Flowability

To determine the flow properties of silica nanoparticle-coated ETZ powders, we obtained the angle of repose and compressibility index using a powder tester (Hosokawa Micron, Osaka, Japan).

The powder flowabilities of sample powders under stress were measured using a direct constant-volume shear tester (NS-S500, Nanoseeds, Nagoya, Japan) with a bottom movable cell (Figure S1). All measurements were made at 25 °C \pm 5 °C and RH = 50% \pm 10% [21,22]. Figure 2 shows the procedure by which NS-S500 measures the powder yield locus (PYL) and consolidation yield locus (CYL) in the powder layer. First, the powder was fed to a height of 25 \pm 5 mm in a stainless-steel cell with an inner diameter of 15 mm and preconditioned under a 5 N vertical load applied at the top of the powder layer. Then, the normal stress on the powder layer was increased to 10 N (P0→P1). After stress relaxation (P1→P2), the powder layer was sheared at 10 $\mu\text{m/s}$ (P2→P3). The procedure was repeated under normal stresses of 15, 20, and 30 N. The shear stress (τ) was plotted as a function of normal stress (σ) (P3). When the shear stress τ reached steady state under a normal stress of 30 N (P2→P3), the normal stress was gradually released by moving the bottom of the powder bed slightly downward (P3→P4) [23]. The PYL curve was obtained by continuously detecting the shear stresses during the process from P3 to P4 (Figure 2). The internal friction angle, shear cohesion, and flow function coefficient (ffc) were determined

by drawing a Mohr's circle corresponding to the PYL. The Mohr circle was obtained with NS-1 (Nanoseeds).

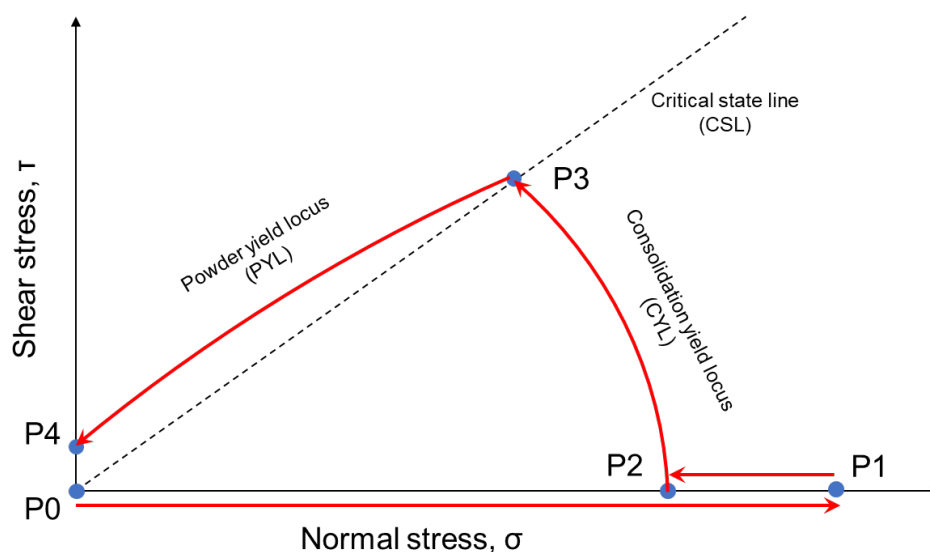


Figure 2. Shear test procedure for powder beds using a Nanoseeds constant-volume-type shear tester (NS-S500) (the procedure is based on Tsunakawa et al. [23]).

2.7. Preparation of ETZ Tablets from Formulated Powder and Evaluation of Tablet Properties

Pharmatose 100M/Ceolus PH-101/ETZ (ETZ coated with silica nanoparticles) were blended in a glass bottle using manual shaking for 1 min. Magnesium stearate was then added and mixed by manual shaking for another 1 min. The final weight ratio of Pharmatose 100M/Ceolus PH-101/ETZ (ETZ coated with silica nanoparticles)/magnesium stearate was 39.5/30/30/0.5. The tablets weighing 200 mg were prepared using a single-punch tableting machine (TK-TB20KN, Tokushu Keisoku, Yokohama, Japan) with flat-faced punches (8 mm diameter). The formulation powder was compressed at 9.85 kN at a compression speed of 1 mm/s. For determining the relative standard deviations (RSDs) in the weights of tablets, the formulated powders were mixed in a V-type powder blender at 30 rpm for 4 min and then powders were tableted at 3 mm/s. The tablets were stored under stabilized conditions in a temperature- and humidity-controlled chamber.

The tablet-crushing load, defining the force required to break a tablet under radial compression, was measured using a portable checker PC-30 (Okada Seiko Co., Ltd.). The tensile strength required for crushing was calculated as follows:

$$\text{tensile strength} = 2F / (\pi DT),$$

where F is the crushing load and D and T are the diameter and thickness of the tablet, respectively.

ETZ dissolution tests were performed using the paddle method (Apparatus 2) described in the Japanese Pharmacopoeia (JP 18th Edition). A sample containing 60 mg ETZ (ETZ coated with silica nanoparticles) was added to 900 mL of distilled water at $37 \text{ }^\circ\text{C} \pm 0.5 \text{ }^\circ\text{C}$ with paddle stirring at 50 rpm. At specific time intervals, 1 mL samples were withdrawn and filtered through a $0.20 \text{ }\mu\text{m}$ sized polytetrafluoroethylene filter. The ETZ concentration in the collected samples was determined in a UV-visible spectrophotometer at 290 nm (UV-1800, Shimadzu, Kyoto, Japan).

3. Result and Discussion

3.1. Particle Morphology and Size Distribution of Ethenzamide Dry Coated with Silica Nanoparticles

Colloidal silica is a commonly used flow enhancer of formulated powders in the pharmaceutical industry. In a preliminary study, we simply mixed silica nanoparticles and ETZ powder mixtures in a common V-shaped lab blender. However, multiple agglomerates

of silica nanoparticles appeared throughout the processed powder. The usual simple mixing process provided insufficient shear stress for effective disaggregation of silica particles and their subsequent van der Waals interactions with the host particles. To improve the flowability of APIs, the mechanical process must provide sufficient shear force while maintaining API properties.

In this study, ETZ was coated with silica nanoparticles using two types of milling equipment: a lab-scale high-speed shear mixer known as Mechanomill (Figure 1a) and a Comil capable of continuous processing. Mechanomill has produced composite particles under dry mechanochemical forces [16,24], whereas Comil has been used for dry coating (Figure 1b). Certain studies on Comil reported the successful dry coating of silica nanoparticles on pharmaceutical excipients [12,13]. Raw powder fed in the Comil is retained in the center of the conical vessel where it is mixed. The conical design and centrifugal forces outwardly push the mixed powder to the tips of the impeller and screen. When the powder is trapped between the screen and impeller edge, the aggregates of silica nanoparticles are disintegrated via shear stress. During this process, the aggregates are supposed to be crushed and preferentially attached to substantially larger host particles via van der Waals interactions.

Figure 3 shows the SEM surface images of ETZ dry coated with different silica nanoparticles in the Mechanomill or Comil mill. Either A200 or R972 nanoparticles coated by Comil were denoted as A200-C and R972-C, respectively, and those coated by Mechanomill were denoted as A200-M and R972-M, respectively. Untreated ETZ appeared as rod-shaped crystals with smooth surfaces (Figure 3a). Both dry-coating processes deposited A200 and R972 silica nanoparticles on the surfaces of ETZ crystals (Figure 3b–e); however, the R972 silica nanoparticles appeared to be more copiously present than 200 silica nanoparticles. Moreover, certain nanoparticles in R972 Comil (R972-C) were clustered owing to the cohesive nature of silica particles (Figure 3d). ETZ particles were neither deformed nor destroyed by the Mechanomill or Comil dry-coating processes. The results suggested that the dry coating of silica nanoparticles on ETZ is feasibly achieved by the shear forces of both types of equipment.

Figure 4 shows the particle size distributions of untreated ETZ and silica-coated ETZ measured by LDSA. The D_{50} of untreated ETZ was 16.24 μm . The particle size distributions of ETZ did not noticeably differ between A200-M and A200-C. Moreover, the ETZ-particle size distribution of R972-C was comparable to that of untreated ETZ, but the D_{50} of R972-M (24.44 μm) was slightly higher than that of untreated ETZ. Shear stress during the Mechanomill process may have caused the agglomeration of certain particles. The longer residence time of powders in the Mechanomill process than in the Comil process allows for a higher shear stress on the powder mixture of silica nanoparticles and drug powder.

Both Mechanomill and Comil milling processes primarily imposed a shear stress on the mixed powder, which effectively disaggregated silica nanoparticles (guest particles) and facilitated their coating on the ETZ (host particles). The mechanochemical energy from the impact in both milling apparatuses enabled the coating of silica nanoparticles without affecting the physical properties of ETZ.

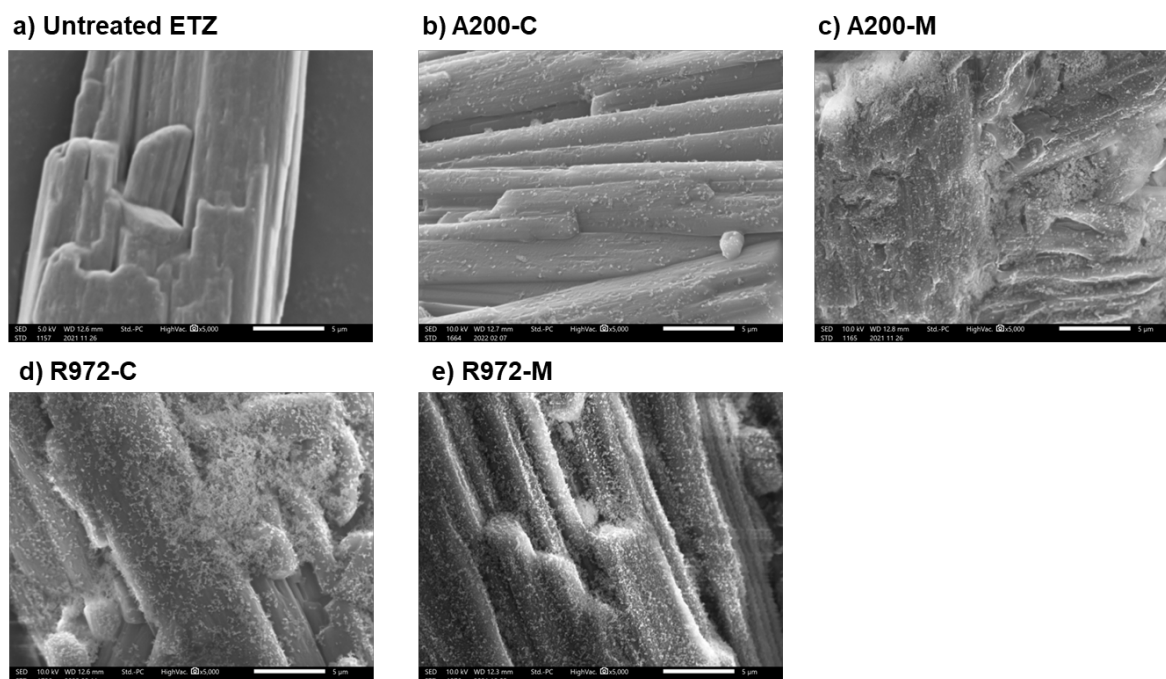


Figure 3. SEM images demonstrating the surface morphologies of ethenzamide (ETZ) particles treated with different types of silica nanoparticles using different dry-coating methods: (a) Untreated ETZ without silica nanoparticles; ETZ coated with A200 silica nanoparticles using the (b) Comil (A200-C) and (c) Mechanomill (A200-M) coating methods; ETZ coated with R972 silica nanoparticles using the (d) Comil (R972-C) and (e) Mechanomill (R972-M) coating methods.

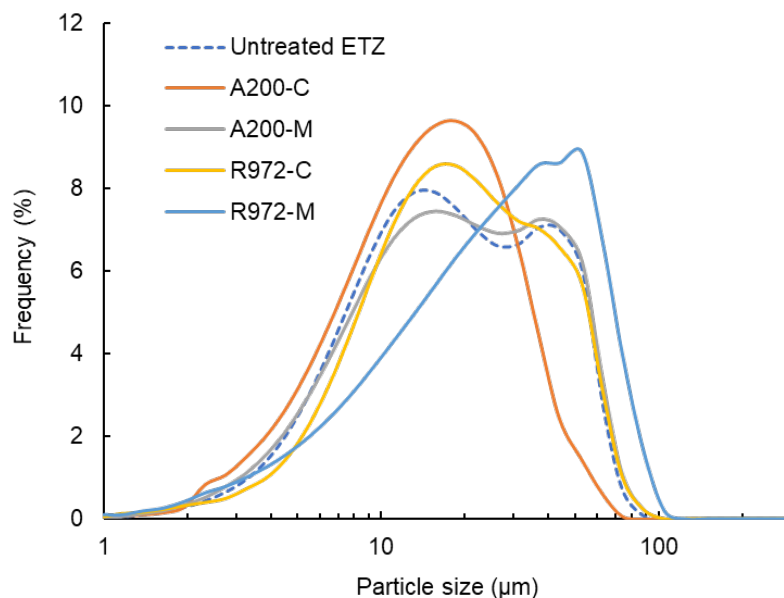


Figure 4. Particle size distributions of ETZ coated with silica nanoparticles using the Mechanomill and Comil methods.

3.2. Static Flowability Evaluation of the Ethenzamide Powder Dry Coated with Silica Nanoparticles

Typically, the flow properties of pharmaceutical powders are determined from the angle of repose, compressibility, and shear cell measurements. The former two parameters provide a static powder flowability index under unstressed conditions, whereas the shear cell method can evaluate the friability and adhesion of powders under stress.

To characterize the effect of dry coating with silica nanoparticles on the flowability of ETZ under unconfined conditions, we determined the angle of repose, bulk density, tap

density, and compressibility using a Hosokawa powder tester (Table 1). The ETZ coated with A200 or R972 demonstrated a higher bulk density and tapped density than untreated ETZ powder, indicating improved powder filling and flowability. Moreover, the silica nanoparticle coating decreased the angle of repose and compressibility, thus, confirming that the coating improved the flowability of ETZ powder. Our results demonstrated that the powder flow properties were improved by both methods of silica nanoparticle surface coating. The primary mechanism of flowability enhancement is physical separation between the host particles by the guest particles attached to the surface [7], which reduces the cohesion. When the cohesion between the particles is sufficiently reduced, the powder flow is considerably improved because gravity on particles can outweigh cohesive forces. Ball-bearing actions of guest particles, such as silica nanoparticles, improve the powder flow by reducing friction between host particles. However, unambiguous differences between the two types of silica nanoparticles and dry-coating methods are difficult to detect from the powder properties of ETZ evaluated using the Hosokawa powder tester.

Table 1. Powder flowability parameters of silica nanoparticle-coated ETZ measured by a Hosokawa powder tester. Data are presented as means \pm standard deviations ($n = 3$).

	Untreated ETZ	A200-C	A200-M	R972-C	R972-M
Angle of repose (degree)	57.37 \pm 1.86	43.70 \pm 1.27	44.30 \pm 0.29	44.37 \pm 0.34	41.30 \pm 0.00
Bulk density (g/cm ³)	0.26 \pm 0.01	0.36 \pm 0.01	0.45 \pm 0.00	0.45 \pm 0.01	0.52 \pm 0.00
Tap density (g/cm ³)	0.56 \pm 0.01	0.61 \pm 0.01	0.70 \pm 0.00	0.68 \pm 0.01	0.75 \pm 0.00
Compressibility (%)	54.2 \pm 3.48	41.50 \pm 0.54	36.03 \pm 0.09	34.30 \pm 0.36	30.23 \pm 0.38

3.3. Surface Free Energy of Silica-Nanoparticle-Coated Ethenzamide Measured by IGC

This study aims to modify the surfaces of APIs by dry coating them with silica nanoparticles. Ultimately, we aimed to improve the powder properties of ETZ. Therefore, we determined the process-induced changes in surface free energies from the total surface energy profiles obtained by IGC (Figure 5a). The total surface energy at zero coverage (corresponding to infinite dilution conditions) was extremely high for untreated ETZ particles but was remarkably lesser after dry coating with either type of silica nanoparticles. The traditional methods of determining the surface energy, such as measuring the contact angle, compute the average surface energies over the entire surface of the material, whereas the surface free energy at infinite dilution in IGC shows only the changes in the highest energy site [20]. The surface-free-energy profile of ETZ coated with silica nanoparticles plateaued at <2% coverage, whereas that of untreated ETZ plateaued at >6% coverage. This result shows a more uniform energy distribution on the surfaces of nanoparticle-coated ETZ than on untreated ETZ. Figure 5b shows the comparison of the ratios of dispersive and Lewis acid–base (polar) components of the total surface free energies among the samples at 10% coverage. Both types of silica nanoparticles reduced the surface free energies of dispersed and polar components. The results demonstrated that silica nanoparticles attached to the ETZ surface decreased the surface free energy and homogenized the surface energy distribution on the crystal surface. Thus, the IGC measurements of surface free energy can determine the success degree of dry-coated silica nanoparticles.

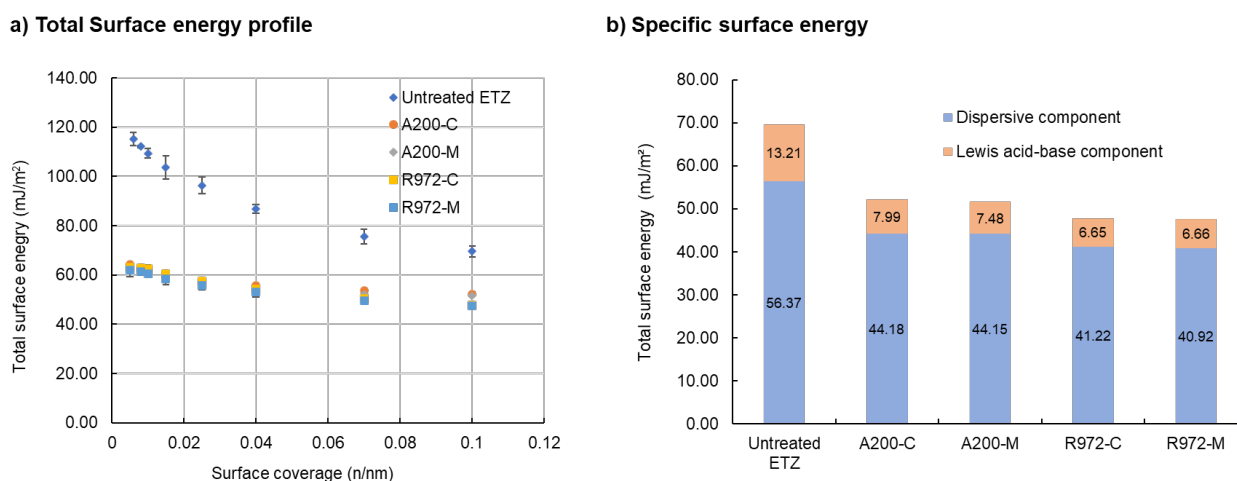


Figure 5. Effect of silica nanoparticle coating on the surface free energy of ETZ: (a) total surface free energies of ETZ powders and (b) proportions of dispersive and polar components of the surface free energies at 10% surface coverage (measured by inverse gas chromatography). In (a), the values are expressed as means \pm standard deviations of the means ($n = 3$).

3.4. Powder Flowability of Ethenzamide Particles Coated with Silica Nanoparticles by the Shear Cell Method

As demonstrated by the results of the Hosokawa powder tester, the mechanochemical forces improved the powder flowability of ETZ coated with silica nanoparticles (Table 1). The flowability parameters (angle of repose, bulk density, and compressibility) determined by the Hosokawa powder tester are effective for evaluating static powder flowability under low stress but are unreliable when applied to sticky powders. Flowability under stress can be evaluated using the shear cell method, which was pioneered by Jenike for hopper and silo design and has become one of the most common powder flow-characterization methods [25,26]. In the shear cell method, a considerable amount of powder spontaneously solidifies under gravity. The flow function coefficient (ffc), cohesion, internal friction angle, and other design parameters can be extracted by analyzing Mohr's stress circle derived from the shear cell test results.

In this subsection, the flowability of ETZ powder was analyzed in a constant-volume shear tester, recently developed by Shimada et al. [21]. NS-S500 is a modified one-surface shear tester that easily yields the PYL and CYL through a single shear test under a constant shear rate after the stress relaxation of the compacted powder layer (Figure 2). In the present shear cell test using NS-S500, the powder was compressed under 30 N (~ 170 kPa, P0 \rightarrow P1 in Figure 2). Then, the normal stress was decreased while maintaining a constant volume for 100 s (P1 \rightarrow P2 in Figure 2). The stress relaxation rate after compression is shown in Figure S2. Dry coating with silica nanoparticles increased the stress relaxation rate of the ETZ powder. The stress gradient developing in the powder layer generates a driving force that causes particles to move. The particles rearrange when the driving force exceeds the adhesion and friction acting between the particles and between the particles and wall, causing plastic deformation within the powder layer. The increased stress relaxation rate suggested that the silica nanoparticle coating encouraged the rearrangement of ETZ particles.

To evaluate the effect of silica nanoparticle coating on the powder properties of ETZ, the internal friction angle, shear adhesion force, and ffc were determined from the Mohr's stress circle tangential to the PYL (Table 2). The dry coating of silica nanoparticles increased the internal friction angle of ETZ. In general, as the inter-particle frictional force increases, the flowability of a powder decreases. The improved flowability of the nanoparticle-coated ETZ was inconsistent with the results of the Hosokawa powder tester (Table 1). In the shear test, the improved mobility of the nanoparticle-coated ETZ particles caused a dense (low porosity) powder layer, in which the apparent internal friction angle was increased by attaching silica nanoparticles to the ETZ. Surface-modified ibuprofen lubricated with a

common lubricant (magnesium stearate) was reported to reduce the inter-particle adhesion by improving the flowability of ibuprofen [6]. The decreased cohesion between particles considerably reduced the internal friction angle of lubricated ibuprofen from that of non-lubricated ibuprofen. Although coating APIs with silica nanoparticles improved their flowability, they increased the inter-particle friction, which may improve the tablet strength under direct compression.

Table 2. Powder flowability parameters of silica nanoparticle-coated ETZ under stress measured by the shear cell method (Nanoseeds constant-volume-type shear tester; NS-S500). Data are presented as means \pm standard deviations ($n = 3$).

	Untreated ETZ	A200-C	A200-M	R972-C	R972-M
Internal frictional angle (degree)	28.97 \pm 1.73	42.43 \pm 1.05	41.93 \pm 1.74	40.00 \pm 0.16	40.47 \pm 0.24
Shear cohesion (kPa)	9.93 \pm 1.31	11.37 \pm 1.76	5.80 \pm 2.67	8.43 \pm 2.65	4.67 \pm 0.94
Flow function coefficient (ffc)	4.07 \pm 0.37	3.60 \pm 0.36	11.03 \pm 5.31	6.50 \pm 2.33	11.93 \pm 4.24

The shear adhesion parameter measured by NS-S500, which reflects the inter-particle adhesion force, was reduced after coating ETZ with silica nanoparticles in the Mechanomill (A200-M and R972-M). The silica nanoparticles uniformly distributed on the surfaces of the ETZ crystals prevented inter-particle adhesion; however, the silica nanoparticles coated by Comil (A200-C and R972-C) did not significantly change the shear adhesion and ffc from those of uncoated ETZ. These results suggested that the silica nanocoating provided by the Comil process was insufficient to improve the powder flowability under stress. Because the bonding between the silica nanoparticles and ETZ surface was lesser in Comil-treated powders (A200-C and R972-C) than in Mechanomill-treated powders, the adhesion between the Comil-treated ETZ particles might not have reduced under stress.

Inadequate dry coating by the Comil process can be attributed to the short residence time of the powder in the impeller zone. Capece and Larson improved the efficiency of dry coating with Comil using a modified screen with a reduced open area [13]. The modified screen increased the average residence time of the powder in the Comil and provided higher powder flowability than the “multi-pass” approach. Therefore, optimizing the process conditions of the Comil might overcome the insufficient dry coating of the ETZ/silica nanoparticles.

3.5. Effect of Dry Coating of Silica Nanoparticles on ETZ Tablet Properties

Comil-prepared ETZ with a dry coating of silica nanoparticles was compressed into tablets (Figure 6). As shown in the results of the shear cell test (Table 2), the improvement degree of the powder properties was greater in the Mechanomill than in the Comil. Therefore, if the single-punch tableting machine can produce tablets of Comil powder, it should produce tablets of Mechanomill powder too. The ETZ content in the tablets was 30%. The relative standard deviations (RSDs) in the weights of untreated ETZ, A200-C, and R972 are compared in Figure 6a. These weight variations were obtained from 100 tablets of each type prepared and collected by continuously feeding raw powder into the feeder of a single-punch tableting machine. The RSDs were significantly lower in tablets of nanoparticle-coated ETZ than in the tablets of untreated ETZ. During tableting, powder flowability is important because if the powder easily and consistently flows into the die, tablets with uniform tablet weight and reproducible properties are obtained. The decreased RSD value after nanoparticle coating was attributed to the improved powder flowability of ETZ attached with silica nanoparticles.

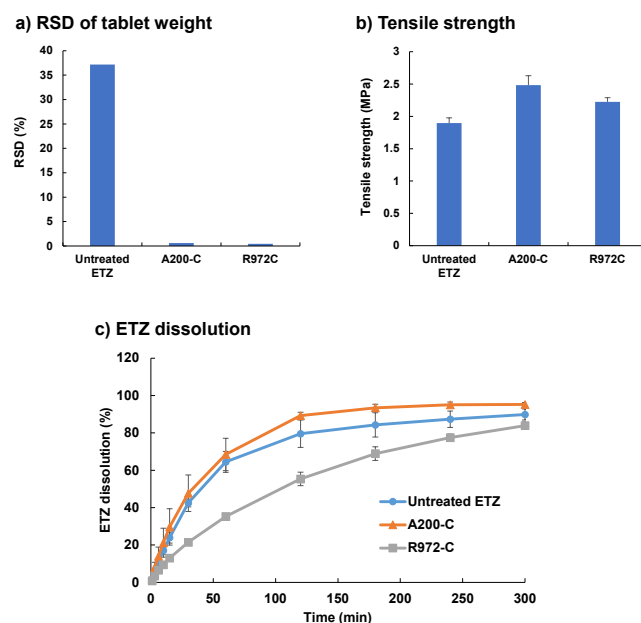


Figure 6. Effect of dry coating of silica nanoparticles by Comil on the properties of ETZ tablets: (a) relative standard deviations (RSDs) of the weights of 50 tablets prepared by a single-punch tableting machine, (b) tensile strengths of the tablets ($n = 5$), and (c) profiles of ETZ dissolution from the tablets ($n = 3$). Values are expressed as means \pm standard deviations of the means.

The tensile strength of ETZ tablets was improved after coating with silica nanoparticles (Figure 6b). Shear test results demonstrated that the silica nanoparticle coating increased the internal friction angle (Table 2), indicating an increased inter-particle bonding force and high tablet hardness.

Figure 6c shows the results of a dissolution test of ETZ from tablets. The dissolution profile of the A200 tablets was similar to that of the untreated ETZ tablets. However, the drug dissolution from ETZ tablets coated with R972 was delayed. A200 has a hydrophilic surface with silanol groups, whereas R972 is rendered hydrophobic by the dimethyl groups on its surface. Therefore, less water is expected to permeate the tablets containing R972. This test demonstrates the possibility of controlling drug dissolution from tablets by changing the physical properties of silica nanoparticles used for dry coating.

The Comil-prepared ETZ with a dry coating of silica nanoparticles was compressed into tablets of uniform weight because nanoparticles improved the powder flowability. However, in the shear cell results (Table 2), the adhesion and flowability of the Comil-prepared nanoparticle-coated ETZ were similar to those of untreated ETZ under stress. In general, powder flowability under stress (which typifies powder behavior in the powder feeder) is important for robust production in scaled-up tablet manufacturing. As Comil operates a continuous process, it is expected to produce more efficient manufacturing than batch-type Mechanomill; however, dry nanocoating by Comil may be insufficient to avoid manufacturing problems. The powder flowability of APIs dry coated with silica nanoparticles under stress could be improved by increasing the residence time of the Comil process for optimizing the impeller shape, rotation speed, screen, and number of passes [13].

4. Conclusions

We attempted to improve the powder properties of an API (specifically, of ETZ powder) by dry coating the powder particles with silica nanoparticles. Both Mechanomill and Comil processes successfully dry coated silica nanoparticles with different physical properties (A200 and R972, respectively) on ETZ crystals. Both silica nanoparticles improved the powder flowability of ETZ (as evaluated by the Hosokawa powder tester) and reduced the surface free energy of ETZ (as measured by IGC). IGC measurements of the surface free energy confirmed that ETZ was dry coated with silica nanoparticles. In shear cell

tests, the flowability under stress of Comil dry-coated powders was comparable to that of untreated ETZ; however, the tablet manufacturing properties of the formulated ETZ can be improved. The batch-wise Mechanomill improved the powder properties in the shear cell test from those of untreated ETZ, suggesting that the process conditions of Comil must be optimized by increasing the residence time of the powder. Although the Comil process requires additional improvements, this study demonstrated the usefulness of Comil as a practical dry-coating process that can improve the properties of API powders.

Supplementary Materials: The following supporting information can be downloaded at: <https://www.mdpi.com/article/10.3390/powders1040016/s1>, Figure S1: Photograph and schematic of the Nanoseeds constant-volume-type shear tester (NS-S500); Figure S2: Stress relaxation during powder compression in the Nanoseeds constant-volume-type shear tester (NS-S500) (P1→P2 sequence in Figure 2).

Author Contributions: Conceptualization, K.T.; methodology, D.Y., M.Y., Y.S. and T.T.; formal analysis, T.T.; investigation, T.T., D.Y., Y.K. and M.Y.; resources, K.T.; data curation, K.T.; writing—original draft preparation, T.T. and K.T.; writing—review and editing, E.Y., T.I. and K.T.; supervision, K.T.; project administration, K.T.; funding acquisition, K.T. All authors have read and agreed to the published version of the manuscript.

Funding: This research was supported by the Knowledge Hub Aichi priority research project (stage III).

Institutional Review Board Statement: Not applicable.

Informed Consent Statement: Not applicable.

Data Availability Statement: Not applicable.

Conflicts of Interest: The authors declare no conflict of interest.

References

1. Leane, M.; Pitt, K.; Reynolds, G.; Manufacturing Classification System Working Group. A proposal for a drug product Manufacturing Classification System (MCS) for oral solid dosage forms. *Pharm. Dev. Technol.* **2015**, *20*, 12–21. [[CrossRef](#)] [[PubMed](#)]
2. Hansen, J.; Kleinebudde, P. Enabling the direct compression of metformin hydrochloride through QESD crystallization. *Int. J. Pharm.* **2021**, *605*, 120796. [[CrossRef](#)] [[PubMed](#)]
3. Han, X.; Ghoroi, C.; To, D.; Chen, Y.; Dave, R. Simultaneous micronization and surface modification for improvement of flow and dissolution of drug particles. *Int. J. Pharm.* **2011**, *415*, 185–195. [[CrossRef](#)] [[PubMed](#)]
4. Leane, M.; Pitt, K.; Reynolds, G.K.; Dawson, N.; Ziegler, I.; Szepes, A.; Crean, A.M.; Dall Agnol, R.; The Manufacturing Classification System McS Working Group. Manufacturing classification system in the real world: Factors influencing manufacturing process choices for filed commercial oral solid dosage formulations, case studies from industry and considerations for continuous processing. *Pharm. Dev. Technol.* **2018**, *23*, 964–977. [[CrossRef](#)] [[PubMed](#)]
5. Morin, G.; Briens, L. The effect of lubricants on powder flowability for pharmaceutical application. *AAPS PharmSciTech* **2013**, *14*, 1158–1168. [[CrossRef](#)]
6. Liu, L.X.; Marziano, I.; Bentham, A.C.; Litster, J.D.; White, E.T.; Howes, T. Effect of particle properties on the flowability of ibuprofen powders. *Int. J. Pharm.* **2008**, *362*, 109–117. [[CrossRef](#)]
7. Sharma, R.; Setia, G. Mechanical dry particle coating on cohesive pharmaceutical powders for improving flowability—A review. *Powder Technol.* **2019**, *356*, 458–479. [[CrossRef](#)]
8. Huang, Z.; Scicolone, J.V.; Han, X.; Dave, R.N. Improved blend and tablet properties of fine pharmaceutical powders via dry particle coating. *Int. J. Pharm.* **2015**, *478*, 447–455. [[CrossRef](#)]
9. Jallo, L.J.; Ghoroi, C.; Gurusurthy, L.; Patel, U.; Dave, R.N. Improvement of flow and bulk density of pharmaceutical powders using surface modification. *Int. J. Pharm.* **2012**, *423*, 213–225. [[CrossRef](#)]
10. Pfeffer, R.; Dave, R.N.; Wei, D.; Ramlakhan, M. Synthesis of engineered particulates with tailored properties using dry particle coating. *Powder Technol.* **2001**, *117*, 40–67. [[CrossRef](#)]
11. Chattoraj, S.; Shi, L.; Sun, C.C. Profoundly improving flow properties of a cohesive cellulose powder by surface coating with nano-silica through comilling. *J. Pharm. Sci.* **2011**, *100*, 4943–4952. [[CrossRef](#)]
12. Mullarney, M.P.; Beach, L.E.; Davé, R.N.; Langdon, B.A.; Polizzi, M.; Blackwood, D.O. Applying dry powder coatings to pharmaceutical powders using a comil for improving powder flow and bulk density. *Powder Technol.* **2011**, *212*, 397–402. [[CrossRef](#)]
13. Capece, M.; Larson, J. Improving the Effectiveness of the Conical Screen Mill as a Dry-Coating Process at Lab and Manufacturing Scale. *Pharm. Res.* **2022**. [[CrossRef](#)]
14. Zhou, Q.; Shi, L.; Marinaro, W.; Lu, Q.; Sun, C.C. Improving manufacturability of an ibuprofen powder blend by surface coating with silica nanoparticles. *Powder Technol.* **2013**, *249*, 290–296. [[CrossRef](#)]

15. Tahara, K. Pharmaceutical formulation and manufacturing using particle/powder technology for personalized medicines. *Adv. Powder Technol.* **2020**, *31*, 387–392. [[CrossRef](#)]
16. Shiino, K.; Iwao, Y.; Fujinami, Y.; Itai, S. Preparation and evaluation of granules with pH-dependent release by melt granulation. *Int. J. Pharm.* **2012**, *431*, 70–77. [[CrossRef](#)]
17. Takeuchi, H.; Nagira, S.; Yamamoto, H.; Kawashima, Y. Solid dispersion particles of tolbutamide prepared with fine silica particles by the spray-drying method. *Powder Technol.* **2004**, *141*, 187–195. [[CrossRef](#)]
18. Jonat, S.; Hasenzahl, S.; Drechsler, M.; Albers, P.; Wagner, K.G.; Schmidt, P.C. Investigation of compacted hydrophilic and hydrophobic colloidal silicon dioxides as glidants for pharmaceutical excipients. *Powder Technol.* **2004**, *141*, 31–43. [[CrossRef](#)]
19. Ho, R.; Heng, J.Y.Y. A Review of Inverse Gas Chromatography and its Development as a Tool to Characterize Anisotropic Surface Properties of Pharmaceutical Solids. *KONA Powder Part. J.* **2013**, *30*, 164–180. [[CrossRef](#)]
20. Karde, V.; Ghoroi, C. Influence of surface modification on wettability and surface energy characteristics of pharmaceutical excipient powders. *Int. J. Pharm.* **2014**, *475*, 351–363. [[CrossRef](#)]
21. Shimada, Y.; Hatano, S.; Matsusaka, S. A new method for evaluating powder flowability using constant-volume shear tester. *Adv. Powder Technol.* **2018**, *29*, 3577–3583. [[CrossRef](#)]
22. Shimada, Y.; Kawata, T.; Matsusaka, S. Analysis of constant-volume shear tests based on precise measurement of stresses in powder beds. *Adv. Powder Technol.* **2018**, *29*, 1372–1378. [[CrossRef](#)]
23. Tsunakawa, H.; Aoki, R. A direct shear test for powders and granular materials. *J. Res. Assoc. Powder Technol. Jpn.* **1974**, *11*, 263–268. [[CrossRef](#)]
24. Honda, H.; Kimura, M.; Honda, F.; Matsuno, T.; Koishi, M. Preparation of monolayer particle coated powder by the dry impact blending process utilizing mechanochemical treatment. *Colloids Surf. Physicochem. Eng. Asp.* **1994**, *82*, 117–128. [[CrossRef](#)]
25. Jager, P.D.; Bramante, T.; Luner, P.E. Assessment of Pharmaceutical Powder Flowability using Shear Cell-Based Methods and Application of Jenike's Methodology. *J. Pharm. Sci.* **2015**, *104*, 3804–3813. [[CrossRef](#)]
26. Salustio, P.J.; Inacio, C.; Nunes, T.; Sousa, E.S.J.P.; Costa, P.C. Flow characterization of a pharmaceutical excipient using the shear cell method. *Pharm. Dev. Technol.* **2020**, *25*, 237–244. [[CrossRef](#)]